Type of submission:

Original Research Paper

Title:

Role of waveform signal parameters in the classification of children as relatively slow and fast myopia progressors in children

Authors and affiliations:

Wan Kin[a], Wolffsohn James Stuart [b], Cho Pauline[a]

[a]School of Optometry, The Hong Kong Polytechnic University, HKSAR, China

[b]School of Optometry, College of Health Life Sciences, Aston University, UK

Running title

Waveform signal and myopia progression

Key words

Myopia, Orthokeratology, Corneal biomechanics

Contact author:

Name: Kin Wan; (+852) 3400 2931; kkinwan@polyu.edu.hk

Address: Optometry Research Clinic, A136-137, School of Optometry, The Hong Kong Polytechnic University, Hung Hom, Kowloon, Hong Kong SAR, China

Abstract

Clinical Relevance: Identification of the baseline characteristics for children undergoing orthokeratology with relatively fast myopia progression can allow a more accurate determination of the risk/benefit ratio.

Background: This study aimed to investigate if baseline corneal biomechanics can classify relatively slow and fast myopia progression in children.

Methods: Children aged six to 12 years with low myopia (0.50 to 4.00 D) and astigmatism (less than or equal to 1.25 D), were recruited. Participants were randomised to be fitted with ortho-k lenses of different compression factors [0.75 D (OK-CCF) n=29 or 1.75 D (OK-ICF) n=33]. Relatively fast progressors were defined as participants who had axial elongation of 0.34 mm or above per two years. A binomial logistic regression analysis and a classification and regression tree model were used in the data analysis. The corneal biomechanics were measured with a bidirectional applanation device. Axial length was measured by a masked examiner.

Results: As there were no significant between-group differences in baseline data (all $p > 0.05$), data were combined for analysis. The mean ± SD axial elongation for relatively slow (n=27) and fast (n=35) progressors were 0.18 ± 0.14 mm and 0.64 ± 0.23 mm per two years, respectively. p2area1 was significantly higher in relatively fast progressors ($p = 0.018$). The binomial logistic regression and classification and regression tree model analysis showed baseline age and p2area1 could differentiate slow and fast progressors over two years.

Conclusions: Corneal biomechanics could be a potential predictor of AE in ortho-k lens wearing children. A further investigation with a larger sample size is warranted

to confirm the applicability of the finding.

Introduction

Axial elongation (AE) is the major structural change affecting myopia development. Studies using animal models have demonstrated that the biomechanics of the posterior ocular tissue are altered during myopia development, with increases in scleral elasticity [1] and extensibility (creep) being observed. [2-4] The biomechanics of the cornea, whose extracellular matrix shares similar composition with posterior ocular tissues, were hypothesized to be able to reflect the biomechanics of posterior ocular tissues [5,6], but this could not be confirmed as it was not feasible to non-invasively measure the biomechanics of posterior ocular tissue.

The bidirectional applanation device (Ocular Response Analyzer, Reichert Ophthalmic Instruments, Buffalo, NY) is a commercially available device, which can measure corneal biomechanics *in vivo* under clinical settings. It generates two corneal biomechanics parameters according to the pressure differences between the first (P1) and second (P2) corneal applanation, namely, corneal hysteresis (CH) and corneal resistance factor (Figure 1). However, determination of corneal hysteresis and corneal resistance factor has a limitation in that they depend on the pressure difference at P1 and P2, so different morphologies of the waveform signal could generate the same corneal hysteresis and corneal resistance factor values. Analysis of the morphologies of the waveform signal could provide additional information compared with only the interpretation of the values of corneal hysteresis and corneal resistance factor. [7] Thirty-seven waveform signal parameters can be generated

according to the morphology of the waveform signal (Table 1).

Severity of myopia and axial length were reported to be associated with corneal hysteresis. [8-12] Several studies have reported that corneal hysteresis is lower in subjects with high myopia. [8, 11-12] In related studies, Song et al. reported that children with longer axial length had a lower corneal hysteresis, [9] Chang et al. observed that the between-eye difference in corneal hysteresis was associated with the between-eye difference in axial length, [10] and Wan et al. demonstrated that lower baseline corneal hysteresis was associated with higher AE in children wearing single-vision spectacles over two years. [13] However, the role of waveform signal parameters in myopia progression has not received any attention.

This study aimed to investigate the role of baseline waveform signal parameters in the classification between relatively fast- and slow-progressors by using a decision tree model.

Methods

This was a longitudinal clinical trial [ClinicalTrials.gov (NCT02643342)] investigating the baseline differences of corneal biomechanics between relatively fast- and slow-progressors. All procedures were performed according to the tenets of the Declaration of Helsinki. Ethics approval was obtained from the Departmental Research Committee of the School of Optometry of The Hong Kong Polytechnic University. Written informed consent was obtained from the parents after thorough explanation of the purpose, nature, and possible consequences.

Healthy children (6 to <12 years old) without prior history of myopia control

93 treatment were recruited. All participants had myopia of 0.50 D to 4.00 D,
94 astigmatism of less than 1.50 D (with-the-rule; ≤ 0.50 D for other axes) in both eyes,
95 and anisometropia of less than 1.00 D. The participants were randomly assigned to
96 two ortho-k groups using either a conventional (OK-CCF; 0.75 D) or increased (OK-
97 ICF; 1.75 D) compression factor (Table 2). Data collection visits were scheduled for all
98 participants at baseline and every six months. All data collection visits were
99 scheduled about the same time of the day (within two hours) as the baseline visit to
100 minimize the potential effects of diurnal variation.
101 Only Ocular Response Analyzer measurements with a waveform score of 4.0 or
102 higher were regarded as valid [14]. The first four measurements (not more than 12
103 consecutive measurements) with the highest waveform score were recorded and
104 averaged. Lenstar LS 900 (Haag-Streit AG, Koeniz, Switzerland) was used to measure
105 central corneal thickness. IOL Master (Carl Zeiss Meditec AG, Germany) was used to
106 measure axial length. The first five consecutive axial length readings (between-
107 reading difference of less than 0.02 mm) were regarded as valid and recorded. [15,16]
108 Axial length measurements were performed by a masked examiner to eliminate
109 potential bias.
110
111 ***Statistical analysis***
112 SPSS software (version 23; IBM Corp., Armonk, NY, USA) was used to
113 perform statistical analysis. The Shapiro-Wilks test was used to test the normality of
114 all data. The baseline between-group differences were tested with unpaired t-tests or
115 Mann-Whitney U tests, as appropriate. Only data from participants (right eye only)

who had completed the whole study with valid Ocular Response Analyzer data were used in the analysis. Only h2, h21, p1area, p1area1, p2area, and p2area1 were used in the analysis since they had been shown to be repeatable (intraclass correlation coefficient > 0.80) in children (Figure 3).[17]

Participants with AE of 0.34 mm or above per two years were defined as relatively fast progressors and the remainder as relatively slow progressors. [18] To determine if baseline characteristics could classify between relatively fast and slow progressors over two years, a binomial logistic regression analysis and the classification and regression tree analysis [19,20] were employed. Classification and regression tree is a decision tree method, using binary splits of all parameters (baseline age, corneal hysteresis, corneal resistance factor, h2, h21, p1area, p1area1, p2area, and p2area1) in the training set. Firstly, a maximal tree was constructed including all parameters. Secondly, trimming was performed to prevent overfitting and a Gini index was used to measure the impurity of the split. The selection of child node depended on the best reduction of the Gini index between the parent and child nodes.[20] The tree model was validated by using a 10-fold cross validation. [21]

Results

The baseline between-group differences in age, refractive errors (spherical equivalence refraction), axial length, central corneal thickness, Goldmann-correlated intraocular pressure, corneal-compensated intraocular pressure, corneal hysteresis, corneal resistance factor, h2, h21, p1area, p1area1, p2area, and p2area1 were not significant (all $p > 0.05$) (Table 3). The mean ± SD age for OK-CCF and OK-ICF were

9.12 ± 1.05 and 9.49 ± 1.08 years, respectively. Since the between-group differences of baseline data were insignificant, the baseline data from both ortho-k groups were pooled together. Twenty-seven participants were classified as relatively slow progressors (AE: 0.18 ± 0.14 mm) and 35 participants as relatively fast (AE: 0.64 ± 0.23 mm) over two years.

For the six waveform signal parameters, only p2area1 was significantly different between relatively slow and fast progressors ($p = 0.018$) (Table 4). A logistic regression model, which consisted of baseline age and p2area1 was statistically significant ($p < 0.001$). The model explained 30.3% (Nagelkerke R^2) of the variance in classification of relatively slow and fast progressors. Increasing age (Odds ratio: 0.391) was associated with a decreased likelihood of being relatively fast progressors, whereas increasing p2area1 (Odds ratio: 1.002, 95% confidence interval: 1.0001 to 1.004) was associated with an increase in the likelihood of being relatively fast progressors.

Figure 4 shows the final classification and regression tree model, which consisted of four nodes. Baseline age was the best predictor and p2area1 was the second predictor to differentiate between relatively slow and fast progressors. The majority (17/20; 85%) of participants with baseline age younger than 8.92 years, were relatively fast progressors. Of the participants older than 8.92 years and with baseline p2area1 lower than 951.39, 88% (14/16) were relatively slow progressors. This model classified 51.9% of relatively slow progressors and 94.3% of relatively fast progressors. The estimated error (standard error) after 10-fold cross-validation was

161 0.44 (0.63).

162

163 **Discussion**

164 The results of this study showed that baseline p2area1 was significantly higher
165 in relatively fast progressors. p2area1 represents the area under the curve of the
166 waveform signal at the second peak (second corneal applanation during Ocular
167 Response Analyzer measurement) and has been previously hypothesized to be
168 related to the ability of cornea to dissipate energy. [22] A larger p2area1 could
169 represent a larger area of corneal applanation, which could indicate a higher amount
170 of energy being stored in the cornea, during the outward corneal movement towards
171 the end of Ocular Response Analyzer measurement. It also implies that greater
172 internal energy was required for the cornea to return to its convex shape. These
173 alterations of energy storage of use suggest that a cornea with larger p2area1 has
174 poorer energy damping abilities. The morphology of the second peak of the
175 waveform signal has been shown to be useful in the diagnosis or detection of
176 multiple ocular conditions, including keratoconus, [23,24] glaucoma, [22] and after corneal
177 cross-linking surgery. [25] According to the binomial logistic regression model, every 10
178 units of p2area1 could result in a 2% increase in odds of being a relatively fast
179 progressor. From the classification and regression tree model, baseline age was the
180 best predictor for AE after two years in a group of ortho-k lens wearing children.
181 Previous studies also showed that participants with younger baseline age tended to
182 progress more rapidly over two years [15,16] and five years. [26] p2area1 could further
183 differentiate between relatively slow and fast progressors, as older children (> 8.92

184 years) with a higher p2area1 (> 951.39) tended to have a higher AE.

185 Although the biomechanics of the cornea differ from those of posterior ocular
186 tissues, corneal biomechanics were hypothesized to be able to reflect the
187 biomechanics of posterior ocular tissues as they share similar extracellular matrix
188 compositions. [5,6] In addition, corneal hysteresis and the morphology of the second
189 peak of the waveform signal have been shown to be related to the stiffness of the
190 sclera. [27,28] A stiffer sclera could yield a smaller area under the second peak of the
191 waveform signal.[28] Mechanical stresses, which act on the eye, especially the
192 posterior ocular tissues, could potentially lead to AE. [29,30] Intraocular pressure is one
193 source of ocular mechanical stress. Elevation of IOP for a short period of time can be
194 caused by many daily life activities. [31-33] An increase in IOP has been suggested to be
195 associated with AE. [34] An eye with a better ability to resist the change induced by
196 mechanical stress could potentially have less AE.

197 The ocular rigidity of myopic eyes has been demonstrated to be lower
198 compared with emmetropic and hyperopic eyes. [35,36] The reduction in the diameter
199 of the scleral collagen fibrils, a lower level of collagen content and proteoglycan
200 synthesis have been suggested to be associated with myopia progression. [1,37-39] The
201 differences in the scleral composition between relatively slow and fast progressors
202 could lead to measurable differences in the waveform signal generated by the Ocular
203 Response Analyzer. This could help to explain why p2area1 may be a potential
204 predictor for AE.

205 In the current study, a decision tree model was adopted. The advantage of this
206 approach is the ability to identify sub-grounds with the highest risk, rather than

focusing on the main effects across the entire sample. [40] The results of both linear regression and the decision tree model indicated that age and p2area1 were potential predictors of AE in ortho-k lens wearing children. Baseline p2area1 differed between relatively slow and fast progressors, which could aid in choice of myopia control interventions. The main limitation for current study was relatively small sample size so that a further stratification of subjects into different age groups to investigate the association between age, p2area1, and myopia progression was not able to perform. It would be worthwhile to carry out further investigations with larger samples of children of different ethnicities to confirm the applicability of the findings.

Acknowledgements

The authors thank Jason Lau for the assistance with Ocular Response Analyzer measurement. The authors also thank Dr Maureen Boost for her advice in the preparation of the manuscript.

References

1 Phillips J, McBrien N. Form deprivation myopia: elastic properties of sclera. *Ophthalmic Physiol Opt* 1995; 15: 357-362.

2 Siegwart Jr JT, Norton TT. Regulation of the mechanical properties of tree shrew sclera by the visual environment. *Vis Res* 1999; 39: 387-407.

3 Phillips JR, Khalaj M, McBrien NA. Induced myopia associated with increased scleral creep in chick and tree shrew eyes. *Invest Ophthalmol Vis Sci* 2000; 41: 2028-2034.

4 Avetisov E, Savitskaya N, Vinetskaya M et al. A study of biochemical and biomechanical qualities of normal and myopic eye sclera in humans of different age groups. *Metab Ophthalmol* 1983; 7: 183-188.

5 Medeiros FA, Meira-Freitas D, Lisboa R et al. Corneal hysteresis as a risk factor for glaucoma progression: a prospective longitudinal study. *Ophthalmol* 2013; 120: 1533-1540.
6 Harper AR, Summers JA. The dynamic sclera: extracellular matrix remodeling in normal ocular growth and myopia development. *Exp Eye Res* 2015; 133: 100-111.
7 Kerautret J, Colin J, Touboul D et al. Biomechanical characteristics of the ectatic cornea. *J Cataract Refract Surg* 2008; 34: 510-513.
8 Shen M, Fan F, Xue A et al. Biomechanical properties of the cornea in high myopia. *Vision Res* 2008; 48: 2167-2171.
9 Song Y, Congdon N, Li L et al. Corneal hysteresis and axial length among Chinese secondary school children: the Xichang Pediatric Refractive Error Study (X-PRES) report no. 4. *Am J Ophthalmol* 2008; 145: 819-826. e811.
10 Chang P-Y, Chang S-W, Wang J-Y. Assessment of corneal biomechanical properties and intraocular pressure with the Ocular Response Analyzer in childhood myopia. *British Journal of Ophthalmology* 2010; 94: 877-881.
11 Jiang Z, Shen M, Mao G et al. Association between corneal biomechanical properties and myopia in Chinese subjects. *Eye* 2011; 25: 1083.
12 Del Buey MA, Lavilla L, Ascaso FJ et al. Assessment of corneal biomechanical properties and intraocular pressure in myopic Spanish healthy population. *J Ophthalmol* 2014; 2014.
13 Wan K, Cheung SW, Wolffsohn JS et al. Role of corneal biomechanical properties in predicting of speed of myopic progression in children wearing orthokeratology lenses or single-vision spectacles. *BMJ open ophthalmology* 2018; 3: e000204.
14 Lam AK, Chen D, Tse J. The usefulness of waveform score from the ocular response analyzer. *Optom Vis Sci* 2010; 87: 195-199.
15 Chen CC, Cheung SW, Cho P. Myopia control using toric orthokeratology (TO-SEE study). *Invest Ophthalmol Vis Sci* 2013; 54: 6510-6517.
16 Cho P, Cheung SW. Retardation of myopia in Orthokeratology (ROMIO) study: a 2-year randomized clinical trial. *Invest Ophthalmol Vis Sci* 2012; 53: 7077-7085.
17 Wan K, Cheung SW, Wolffsohn JS et al. Repeatability of corneal biomechanics waveform signal parameters derived from Ocular Response Analyzer in children. *Cont Lens Anterior Eye* 2021; 44: 101373.

18 Cheung S-W, Boost MV, Cho P. Pre-treatment observation of axial elongation for evidence-based selection of children in Hong Kong for myopia control. *Contact Lens and Anterior Eye* 2019; 42: 392-398.

19 Lemon SC, Roy J, Clark MA et al. Classification and regression tree analysis in public health: methodological review and comparison with logistic regression. *Annals of behavioral medicine* 2003; 26: 172-181.

20 Breiman L, Friedman JH, Olshen RA et al. *Classification and regression trees*: Routledge, 2017.

21 Friedman JH. *The elements of statistical learning: Data mining, inference, and prediction*: Springer, 2017.

22 Aoki S, Murata H, Matsuura M et al. The relationship between the waveform parameters from the ocular response analyzer and the progression of glaucoma. *Ophthalmol Glaucoma* 2018; 1: 123-131.

23 Luz A, Fontes BM, Lopes B et al. ORA waveform-derived biomechanical parameters to distinguish normal from keratoconic eyes. *Arq Bras Oftalmol* 2013; 76: 111-117.

24 Ventura BV, Machado AP, Ambrósio Jr R et al. Analysis of waveform-derived ORA parameters in early forms of keratoconus and normal corneas. *J Refract Surg* 2013; 29: 637-643.

25 Spoerl E, Terai N, Scholz F et al. Detection of biomechanical changes after corneal cross-linking using Ocular Response Analyzer software. *J Refract Surg* 2011; 27: 452-457.

26 Hiraoka T, Kakita T, Okamoto F et al. Long-term effect of overnight orthokeratology on axial length elongation in childhood myopia: a 5-year follow-up study. *Invest Ophthalmol Vis Sci* 2012; 53: 3913-3919.

27 Taroni L, Bernabei F, Pellegrini M et al. Corneal biomechanical response alteration after scleral buckling surgery for rhegmatogenous retinal detachment. *Am J Ophthalmol* 2020; 217: 49-54.

28 Roberts CJ. Corneal hysteresis and beyond: Does it involve the sclera? *J Cataract Refract Surg* 2021; 47: 427-429.

29 Greene PR. Mechanical considerations in myopia: relative effects of accommodation, convergence, intraocular pressure, and the extraocular muscles. *Am J Optom Physi Optic* 1980; 57: 902-914.

30 McMonnies CW. Intraocular pressure spikes in keratectasia, axial myopia, and glaucoma. *Optom Vis Sci* 2008; 85: 1018-1026.

31 Bakke EF, Hisdal J, Semb SO. Intraocular pressure increases in parallel with systemic blood pressure during isometric exercise. *Invest Ophthalmol Vis Sci* 2009; 50: 760-764.
32 McMonnies CW, Boneham GC. Corneal curvature stability with increased intraocular pressure. *Eye Cont Lens* 2007; 33: 130-137.
33 Gandhi PD, Gürses-Özden R, Liebmann JM et al. Attempted eyelid closure affects intraocular pressure measurement. *Am J Ophthalmol* 2001; 131: 417-420.
34 Greene PR, McMahon TA. Scleral creep vs. temperature and pressure in vitro. *Exp Eye Res* 1979; 29: 527-537.
35 Berisha F, Findl O, Lasta M et al. A study comparing ocular pressure pulse and ocular fundus pulse in dependence of axial eye length and ocular volume. *Acta Ophthalmol* 2010; 88: 766-772.
36 Lam AK, Wong S, Lam CS et al. The effect of myopic axial elongation and posture on the pulsatile ocular blood flow in young normal subjects. *Optom Vis Sci* 2002; 79: 300-305.
37 Rada JA, Nickla DL, Troilo D. Decreased proteoglycan synthesis associated with form deprivation myopia in mature primate eyes. *Invest Ophthalmol Vis Sci* 2000; 41: 2050-2058.
38 McBrien NA, Gentle A. Role of the sclera in the development and pathological complications of myopia. *Prog Retin Eye Res* 2003; 22: 307-338.
39 He M, Wang W, Ding H et al. Corneal biomechanical properties in high myopia measured by dynamic scheimpflug imaging technology. *Optom Vis Sci* 2017; 94: 1074-1080.
40 Fernández L, Mediano P, García R et al. Risk factors predicting infectious lactational mastitis: decision tree approach versus logistic regression analysis. *Matern Child Health J* 2016; 20: 1895-1903.

Corresponding author:

Name: Kin Wan; (+852) 3400 2931; kkinwan@polyu.edu.hk

Address: Optometry Research Clinic, A136-137, School of Optometry, The Hong Kong Polytechnic University, Hung Hom, Kowloon, Hong Kong SAR, China

Table 1. Summary and definitions of Ocular Response Analyzer waveform signal parameters.

Parameters		
Peak 1	**Peak 2**	**Definition**
slew1	slew2	ratio between dive1/2 and w1/2
mslew1	mslew2	maximum single continuous increase in the rise
dive1	dive2	backside of downslope of peak until first break
aindex	bindex	the smoothness of the peak,
alphf		the smoothness of the signal between the peaks
p1area, p1area1	p2area, p2area2	area under the curve
h1, h11	h2, h21	height of the peak
w1, w11	w2, w21	width of the peak, descriptor of the time course
aspect1,	aspect2,	aspect ratio of the peak
uslope1,	uslope2,	rate of increase from base to peak
dslope1,	dslope2,	rate of decrease from peak to base
path1, path11	path2, path21	the path length around the peak

340 **Table 2.** Characteristics of orthokeratology lenses used in current study.

Manufacturer	NKL Contactlenzen
Material	Siloxanylstyrene fluoromethacrylate
Design	Parallel reverse geometry
Back optic zone radius (mm)	7.2 - 9.50 (0.05 mm step)
Back optic zone diameter (mm)	6
Lens power	Plano
Compression factor (D)	0.75(OK-CCF)/1.75(OK-ICF)
Overall lens diameter (mm)	10.2/10.6/11.00
Tangential angle (degree)	50 - 65 (1^{o} step)
Peripheral Curve	Tangential periphery
Sagittal depth (mm)	0.50 - 0.99 (0.01 mm step)
Central thickness (mm)	0.24

341 OK-CCF: conventional compression factor group; OK-ICF increased compression
342 factor group
343

Table 3. Baseline data in groups wearing orthokeratology lenses with conventional compression factor (OK-CCF, 0.75 D) and increased compression factor (OK-ICF, 1.75D).

	OK-CCF (n=29)	OK-ICF (n=33)	P*
Age, year	9.12 ± 1.05	9.49 ± 1.08	0.175
SER, D	-2.34 ± 0.76	-2.39 ± 0.93	0.805
AL, mm	24.34 ± 0.66	24.47 ± 0.83	0.498
CCT, μm	548.00 ± 28.83	548.03 ± 29.35	0.997
IOPg, mmHg	14.66 ± 3.46	14.23 ± 2.60	0.587
IOPcc, mmHg	15.83 ± 3.18	15.20 ± 2.66	0.399
CH, mmHg	9.87 ± 1.49	10.13 ± 1.39	0.486
CRF, mmHg	9.71 ± 1.75	9.80 ± 1.44	0.813
h2	354.67 ± 51.64	383.51 ± 77.06	0.093
h21	236.45 ± 34.43	255.67 ± 51.37	0.086
p1area	4111 ± 733	4241 ± 1,054	0.581
p1area1	1725 ± 345	1855 ± 502	0.246
p2area	2331 ± 636	2523 ± 693	0.262
p2area1	999 ± 287	1100 ± 321	0.199

Data are presented as mean ± SD or median (range).

SER: spherical equivalence refraction, AL: axial length, CCT: central corneal thickness, IOPg: Goldmann-correlated intraocular pressure, IOPcc: corneal-compensated intraocular pressure, CH: corneal hysteresis, CRF: corneal resistance factor

*Probability values of unpaired t-test for between-group difference.

354 **Table 4.** Baseline data in relatively slow progressors and relatively slow progressors

	Slow (n=27)	Fast (n=35)	P*
Age, year	9.81 ± 0.86	8.94 ± 1.08	0.001
CCT, µm	542 ± 29.58	553 ± 27.87	0.156
IOPg, mmHg	14.93 ± 3.03	14.05 ± 2.99	0.256
IOPcc, mmHg	16.03 ± 3.15	15.08 ± 2.68	0.201
CH, mmHg	9.91 ± 1.30	10.09 ± 1.54	0.636
CRF, mmHg	9.82 ± 1.32	9.71 ± 1.77	0.781
h2	363.57 ± 70.34	374.99 ± 65.73	0.513
h21	242.38 ± 46.89	249.99 ± 43.82	0.513
p1area	4138 ± 1124	4213 ± 725	0.753
p1area1	1795 ± 553	1793 ± 330	0.987
p2area	2273 ± 648	2555 ± 667	0.100
p2area1	966 ± 291	1147 ± 292	0.018

355 Data are presented as mean ± SD.

356 CCT: central corneal thickness, IOPg: Goldmann-correlated intraocular pressure,

357 IOPcc: corneal-compensated intraocular pressure, CH: corneal hysteresis, CRF:

358 corneal resistance factor

359 *Probability values of unpaired t-test for between-group difference.

360

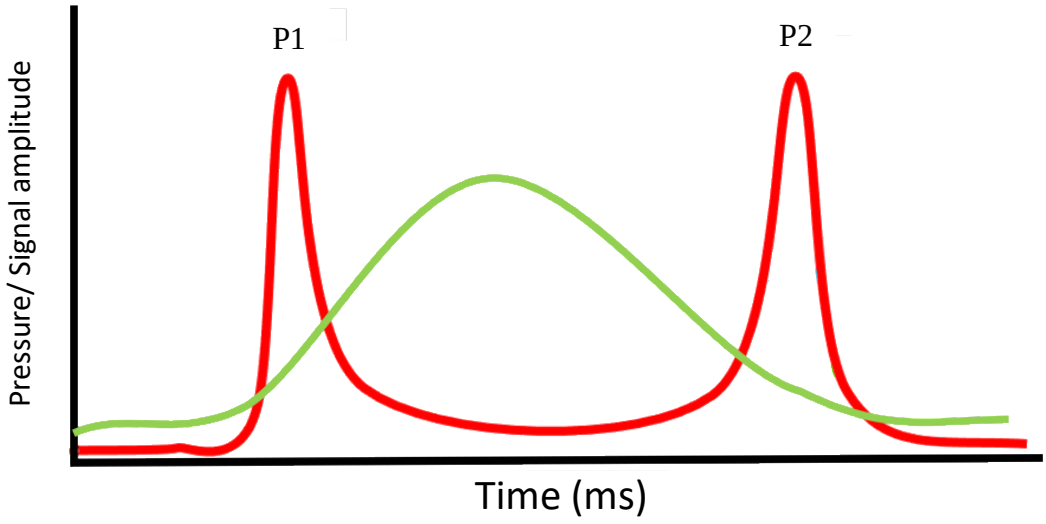

Figure 1. The double-peak waveform of the Ocular Response Analyzer signal. Green line: pressure of the air-puff; Red line: infrared signal; P1: first corneal applanation (peak 1); P2: second corneal applanation (peak 2).

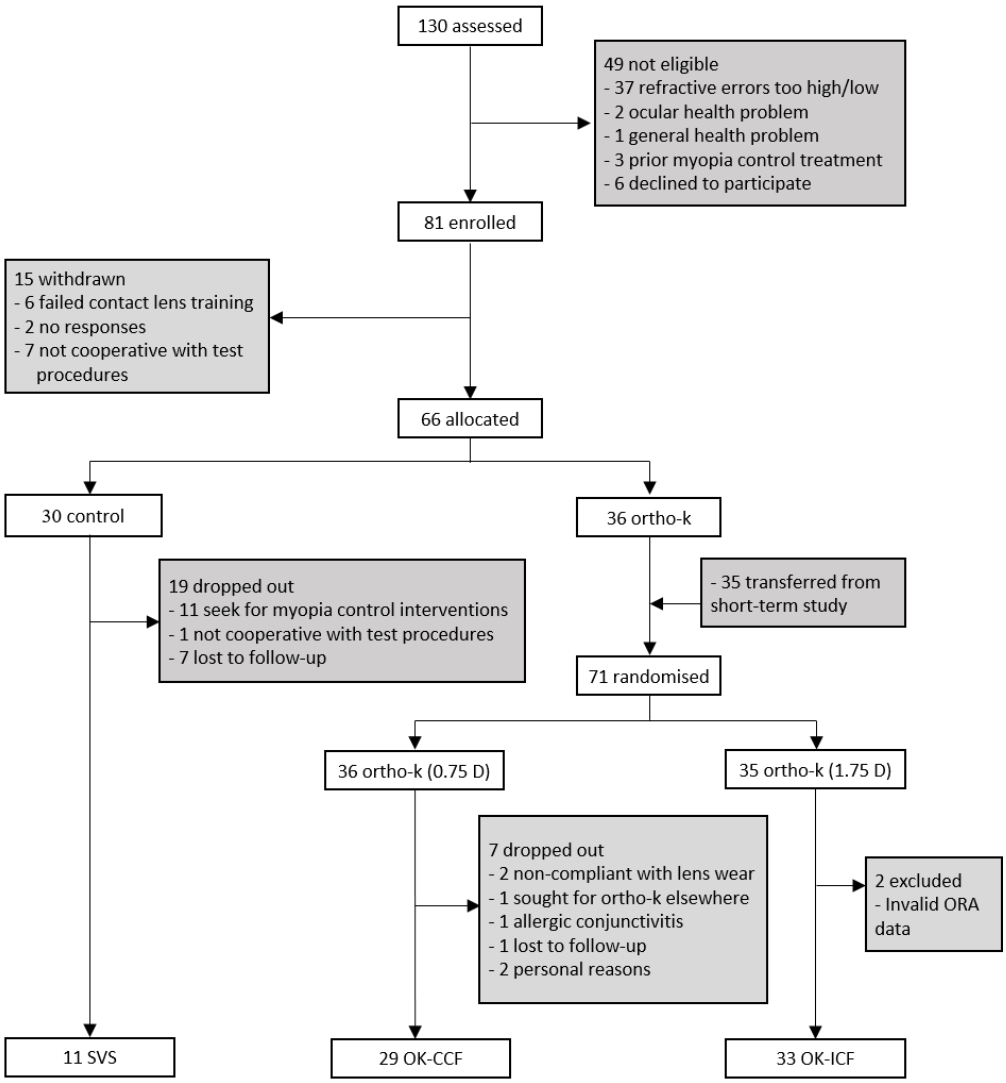

Figure 2. Study flowchart.

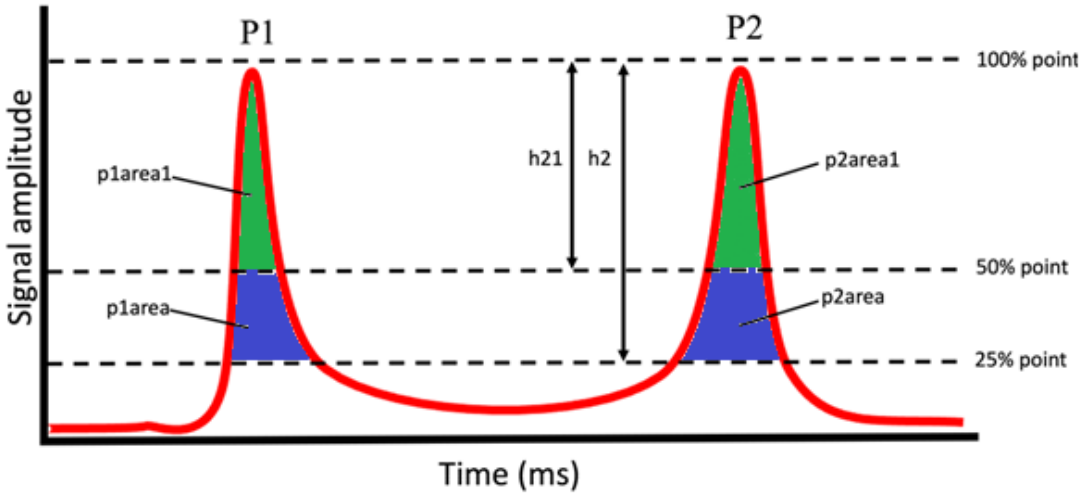

370

371 **Figure 3.** Illustration of waveform signal parameters (h2, h21, p1area, p1area1,
372 p2area, and p2area1). P1: first corneal applanation (peak 1); P2: second corneal
373 applanation (peak 2).

374

375

376

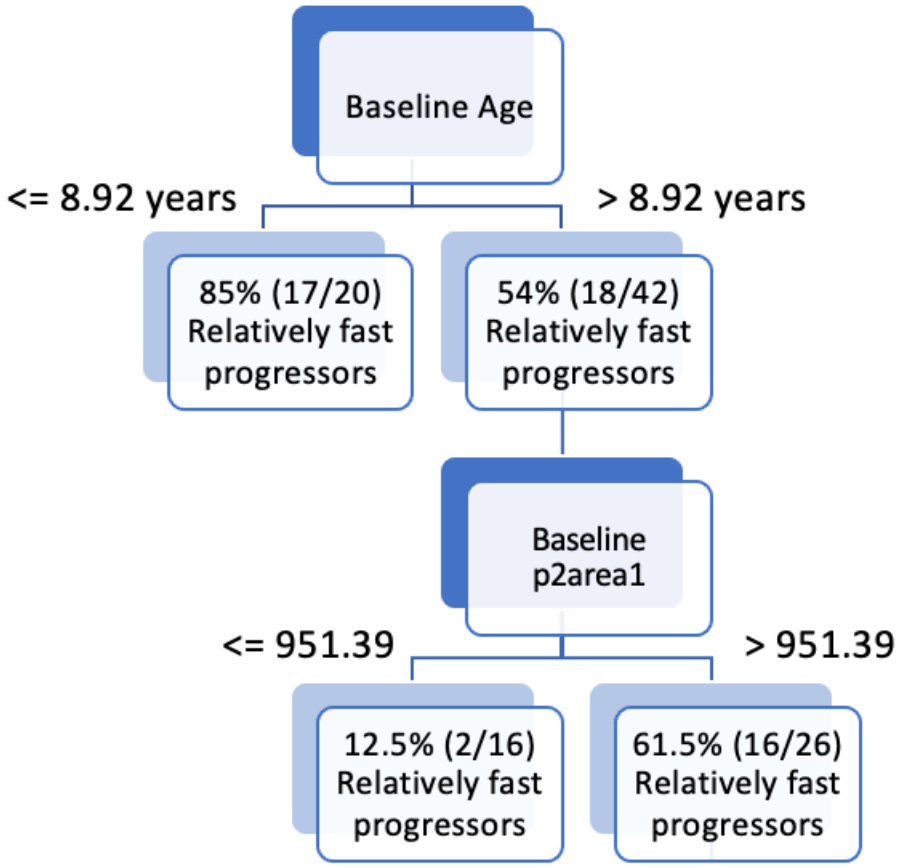

Figure 4. The classification tree of relatively fast and slow progressors using the classification and regression tree model.